Mon. Not. R. astr. Soc. (1988) **231,** 695–722

Spectropolarimetry of SN 1987A: observations up to 1987 July 8

Mark Cropper,* Jeremy Bailey, J. McCowage, R. D. Cannon, Warrick J. Couch, J. R. Walsh, J. O. Strade and F. Freeman *Anglo-Australian Observatory, PO Box 296, Epping, NSW 2121, Australia*

Accepted 1987 September 23. Received 1987 September 11

Summary. We present spectropolarimetric observations of SN 1987A in the LMC. These are the first such observations of a supernova with a signal-to-noise ratio sufficient to show polarization variations across the spectral lines. Observations have been made at several epochs and cover a number of spectral regions; in most cases these include the region around Hα. In general the polarization through the lines is double peaked above a continuum value. We discuss in some detail the interstellar component in order to investigate its effect on the polarization profile. The presence of polarization shows that the supernova explosion was asymmetric. The axis and degree of asymmetry is dependent on wavelength. We interpret our observations in terms of existing models but more detailed modelling will be needed to obtain full agreement with the observed polarization spectrum. We also investigate whether the position angle of the polarization may be related to the position of the companion source observed using speckle interferometry. The principal symmetry axis of the supernova envelope appears to be aligned with the angle to the speckle companion.

We also describe the modifications made to the existing spectropolarimetry on the Anglo-Australian Telescope in order to obtain the high signal-to-noise ratios required for the observations.

1 Introduction

When SN 1987A was discovered the opportunity arose for a number of different types of observations which were at best only marginally possible for previous supernovae. One of these was spectropolarimetry at a high signal-to-noise (S/N) ratio. The Anglo-Australian Telescope is the only telescope from which the supernova is accessible and which has the necessary instrumentation to make these observations (although some modifications were required to the existing IPCS-based spectropolarimeter which was optimized for much fainter objects).

*Present address: Mullard Space Sciences Laboratory, Holmbury St Mary, Dorking, Surrey RH5 6NT.

We present here the spectropolarimetric observations we have carried out up to 1987 July 8. Preliminary reports have been published in Walsh, Bailey & Ogura (1987), Couch *et al.* (1987) and in Bailey, Cannon & Cropper (1987). Observations will continue to be made and will be published in subsequent papers, but we believe that it is important to make available to the astronomical community the large body of data we have already acquired. In the same spirit, the urgency of making the data available precludes any modelling of our results in this paper; we have simply interpreted our results in the light of existing models. In addition we have taken the opportunity for discussing the effects of various complicating factors (for example intervening dust) and commented on the nature of the companion detected by speckle observations.

As pointed out by McCall (1984), spectropolarimetry of supernovae promises to provide important information on the processes occurring during the outburst: it has consequences for the distance scale and also provides stronger and different constraints on the physical processes occurring in the expanding atmosphere than do the line profiles themselves. The subject is very new, both observationally (these are the first successful spectropolarimetric observations reported) and theoretically. Nevertheless we believe that these results will provide the spur for further research on the subject.

2 Observations

We have obtained polarimetric observations of SN 1987A on a variety of occasions using two different instrumental set-ups. The first used the AAT spectropolarimeter with the IPCS as detector (McLean *et al.* 1984) to obtain spectropolarimetry in the 3400–5300 Å range on February 27, four nights after discovery. However, it was clear from the outset that the counting rate limitations of the IPCS would severely limit the degree of accuracy which could be obtained in a reasonable length of time. Therefore a new observing configuration was developed for the spectropolarimeter so that it could use the GEC and RCA CCDs as detectors. This has enabled us to measure polarization in the spectrum at high S/N ratios. The new instrument is described in Section 3 below. As an indication of its performance we show in Fig. 1 spectropolarimetry of the Serkowski (1974) standard *o* Sco (HD 147084) which has a measured polarization of 4.3 per cent at 6800 Å with a position angle of 32°. The polarization spectrum shows no excursions larger than those expected from photon statistics over this range and is in excellent agreement with the standard values.

We have made observations with this configuration on four separate occasions. Our first observations were taken on March 7. They were followed by a two-month gap, after which observations were made roughly every four weeks on May 5, June 3 and June 28. The June 28 observations were taken under very poor conditions. Further observations were taken with the RCA CCD on July 3, 4 and 5 in the blue and with the GEC CCD on July 8 in the red.

Table 1 provides a log of our spectropolarimetric observations and also lists the instrumental set-up, wavelength regions covered and observer. When the spectropolarimeter was first adapted to use a CCD as detector, we concentrated on the strong Hα line. In order to provide a record of the evolution of this line profile it has been observed at subsequent epochs whenever possible. Because the polarization of this profile had increased so markedly between the March and May observations, we decided that observations of other lines would be both feasible and important. We therefore increased the spectral coverage for subsequent observations.

The large zenith distance of the supernova during June and July meant that a few observations had to be made with the telescope mirror partially occulted by the dome. Comparison of these observations with others in the same wavelength region shows that this does not appear to have had any substantial effect on the polarization. At worst, it should only shift the mean level of the polarization and would not affect the differential measurement of the polarization through the lines.

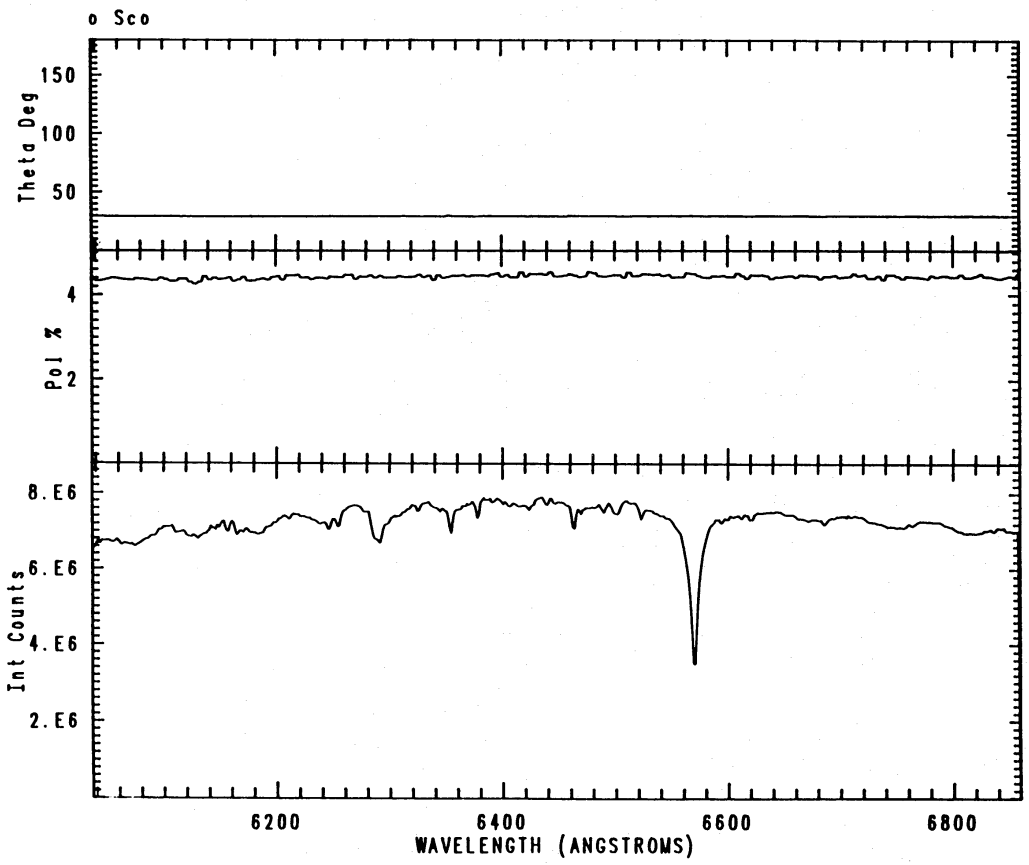

Figure 1. Spectropolarimetry of the Serkowski (1974) standard *o* Sco in the Hα region, using the GEC CCD. The measured polarizations for this A5II–III star at 6800 Å are 4.3 per cent at 32°. Our measurements are in excellent agreement.

Table 1. Log of the spectropolarimetric observations taken on the AAT.

Date	Detector	Camera	Wavelengths	Grating	Type	Observer
1987 Feb 27	IPCS	82cm	3450 – 5300Å		linear	JRW
1987 Mar 7	GEC CCD	82cm	6000 – 6540Å	270R	linear	WJC
		82cm	6260 – 6800Å	270R	linear	WJC
1987 May 5	GEC CCD	25cm	6040 – 6840Å	600R	linear	MSC
1987 Jun 3	GEC CCD	25cm	5440 – 6260Å	600R	linear	RDC
			6040 – 6840Å	600R	linear	JAB+RDC
			8220 – 9050Å	600R	linear	JAB+RDC
1987 Jun 28	GEC CCD	25cm	6040 – 6840Å	600R	linear	MSC
			6040 – 6840Å	600R	circular	MSC
1987 Jul 3	RCA CCD	82cm	3610 – 4340Å	250B	linear	JAB
			4270 – 5000Å	250B	linear	JAB
1987 Jul 4	RCA CCD	82cm	4860 – 5580Å	250B	linear	JAB
1987 Jul 5	RCA CCD	82cm	5440 – 6160Å	250B	linear	JAB
1987 Jul 8	GEC CCD	82cm	6100 – 6600Å	270R	linear	MSC+JAB
			6100 – 6600Å	270R	circular	JAB+MSC
			8300 – 8800Å	270R	linear	JAB+MSC
			8300 – 8800Å	270R	circular	MSC+JAB

3 The CCD spectropolarimeter

The RGO spectrograph+Pockels cell+IPCS is a well-proven spectropolarimeter on the AAT (McLean *et al.* 1984). It has low instrumental polarizations and can be used to measure both linear and circular polarizations. However, the count-rate limitations of the IPCS (~1 count s^{-1} $pixel^{-1}$)

require that neutral-density filters are placed in the beam for objects brighter than $B \simeq 14$ when working at low resolution. When the width of the spectra on the detector in the spatial direction is taken into account, the count rate is limited to ~5 count s^{-1} per spectral element and in order to reach a total count N per spectral element of 10 000 counts, ~1000 s exposure are required (since there are two spectra on the detector corresponding to the Ordinary and Extraordinary rays). The photon error in the polarization is $\sqrt{(2/N)}$ and after 1000 s this is ~1.4 per cent. Binning in the spectral direction is therefore essential to reduce the photon errors; however, binning by a factor of 10 only reduces the uncertainty to ~0.5 per cent per bin. Further binning and longer exposures may be possible but it is impossible to reduce the photon error by more than a relatively small factor within a reasonable observing time. In the case of SN 1987A, this problem is exacerbated by the fact that count rates at the peak of the emission profile and the centre of the absorption trough can differ by factors of 5 or more, and the level of the V-band polarization is <1.0 per cent. It is clear that the count-rate limitation on the IPCS provides a serious obstacle to obtaining spectropolarimetry with sufficient S/N ratios to be useful.

In order to circumvent these difficulties, we adapted the spectropolarimeter to use the GEC and RCA CCDs as detectors. In the IPCS version of the instrument the Pockels cell switches state from + to − quarter-wave retardance every second. The CCDs do not provide any straightforward way of recording both states of this rapid modulation. The solution adopted is to slave the shutter to the switching of the Pockels cell, so that a given CCD exposure records data in only one Pockels cell state. The exposure may be as long as required to achieve a satisfactory signal, as the shutter continues to open each time the Pockels cell switches to the desired state. This exposure is then read out and a second exposure is made in the opposite Pockels cell state. Software has been developed, running under the VAX ADAM system, to perform such a pair of exposures automatically with any required exposure time.

This method has the drawback that the time spent recording data is less than 50 per cent. However, this is more than made up for by the increased photon detection rate. For a third magnitude object with the 25-cm camera and 600-line grating covering 800 Å at a time, we found that typical exposures of 4 s (corresponding to 20 s of elapsed time) produced images at roughly half the saturation level (30 000 ADU or 110 000 e^-). Even accounting for a further 80 s for readout time, this resulted in a gain in observing efficiency over the IPCS of ~100 or more. The CCD system results in a very slow modulation, compared with the 1-s rate obtained using the IPCS. However, this is not a problem in practice as the polarizations are measured *simultaneously* in both the E and O rays, and can therefore be reduced in such a way that seeing or transparency variations between the A and B state observations have little effect on the derived polarization.

Our standard observing procedure is to make linear polarization observations in the Q and U Stokes parameters (obtained by inserting quarter-wave plates in front of the Pockels cell modulator), and then to repeat the observations with the entire instrument rotated through 45°. This helps to correct for residual systematic errors in the polarimetry. For circular polarization observations two instrument rotator positions 90° apart are used.

Standard stars of known polarization were also observed each night. In most cases this included a polarized and an unpolarized standard. Because almost as much time was required to obtain high S/N polarizations for the standards as for SN 1987A, these overheads were minimized by observing the standards in the 6040–6840 Å range only.

4 Reductions

Each pair of A and B state frames was reduced independently. The E and O ray spectra for the star and sky apertures on this image were summed in the spatial direction and the CCD bias level was subtracted. The E spectra of each AB frame pair were then summed and divided by the sum

of the O spectra. The O spectrum in each of the A and B states was multiplied by the resultant ratio spectrum. The sky spectra for each state were subtracted from the star data. The polarized flux for each ray was then determined by subtracting the A and B state spectra. The total intensity spectra in each ray were also generated from the sum of the A and B state spectra. The polarization in each Stokes parameter was then calculated from the ratio of the mean of the polarized flux spectra for the E and O rays to the mean of the intensity spectra for the two rays. This procedure allows for the difference in total counts in the A and B state spectra because of different observing conditions as mentioned in Section 3.

The polarization and intensity spectra from the two spectrograph rotations were combined. Finally, the spectra were rebinned on to a linear wavelength scale determined from CuAr arcs (in some cases CuHe and FeAr arcs were also used), and the Q and U Stokes parameters transformed into the linear polarization p and its position angle θ.

The reliability of the data were checked by comparing the results from independent frame pairs obtained for the same Stokes parameter. Good agreement was found even in cases where large intensity changes had occurred between the A and B state observations. Observations of polarized standard stars show good agreement with their catalogued values, while unpolarized standard stars show observed levels of at most 0.05 per cent.

5 Comments on the reduced spectra

The reduced observations are shown in Figs 2 to 15. In each case the lowest panel of these figures shows the total intensity on a linear scale. The next shows the linear polarization, the third its position angle while Figs 3 to 15 also have a fourth panel showing the polarized flux. The linear polarization has been binned in wavelength so that the standard error on the polarization is 0.3 per cent for Fig. 2 and only 0.05 to 0.08 per cent for Figs 3 to 15. The intensity spectrum in these observations has not been placed on a flux scale.

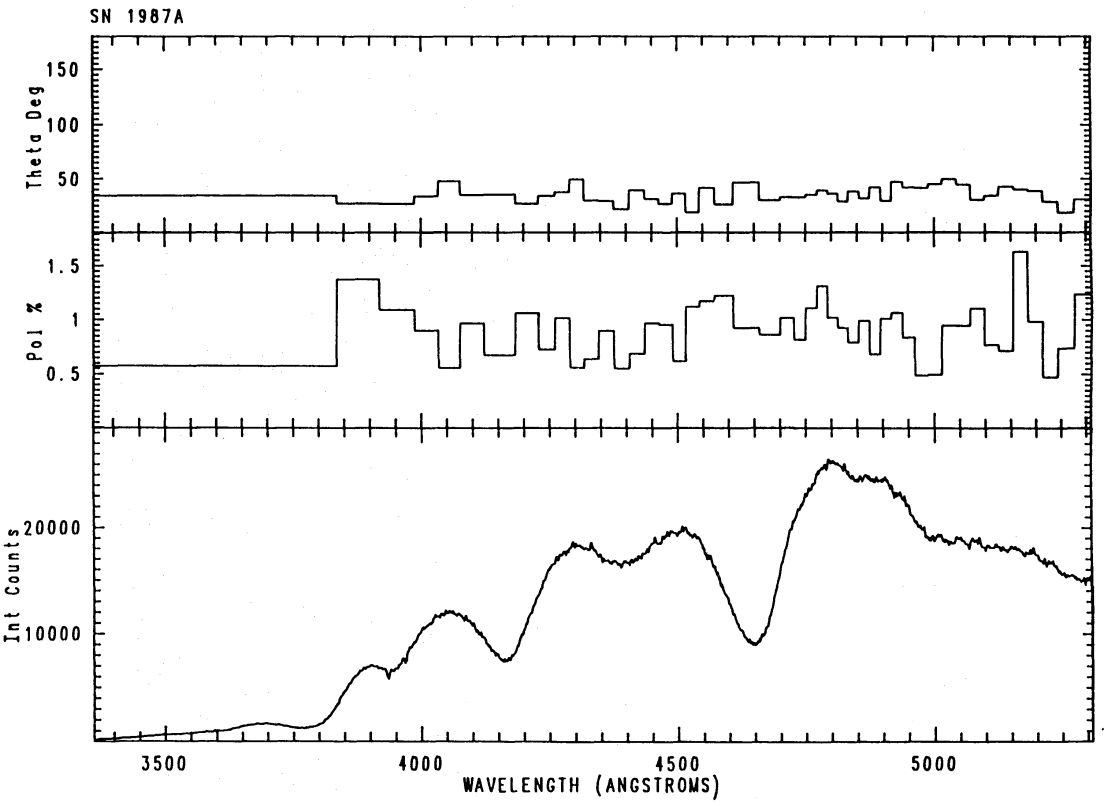

Figure 2. Spectropolarimetry of SN 1987A on February 27 in the blue using the IPCS as detector.

No strong polarization features are visible in the blue spectrum taken only four days after discovery. Using the GEC CCD, however, our S/N ratios are higher and on March 7 we found a flat polarization spectrum with a small dip in the polarization and position angle centred on 6300 Å, just to the blue of the centre of the Hα absorption trough (Figs 3 and 4). Because the dispersion of the 82-cm camera is high we covered the wavelength range in two steps. We saw the feature at both grating angles, leaving no doubt as to its reality, and the agreement between the measured polarizations is excellent.

By May 5 (Fig. 5), considerable evolution of the polarization spectrum had occurred. The polarization profile through Hα had become double humped, while the position angle generally increased through the emission peak. The level of the continuum polarization had dropped from ~0.8 per cent to ~0.5 per cent, and the polarization rose to 1.4 per cent at the blue peak. We obtained enough wavelength coverage to include the line at 6160 Å which showed a rapid change in position angle at the centre of the absorption trough.

Although we have no observations between March 7 and May 5, narrow-band filter observations by Magalhaes & Velloso (1987) show that increased polarization on Hα was present as early as March 21.

After May 5 it was clear that spectropolarimetry at other wavelengths was also important. Therefore on June 3 we obtained the Hα profile (shown in Fig. 7) and an overlapping spectral region to the blue covering the Na *D* lines (Fig. 6). In addition, we covered the Ca II triplet at 8800 Å (Fig. 8). The Hα appears to be evolving in a consistent manner – the continuum polarization has dropped to even lower levels and the polarization through the line has increased to nearly 2.3 per cent. The position angle variation through the line is similar to that found on May 5, but rises more steeply. The polarization of the line at 6160 Å has also increased. The position angle to the blue of Hα looks ragged because it passes through 0° and reappears at 180°. The blue

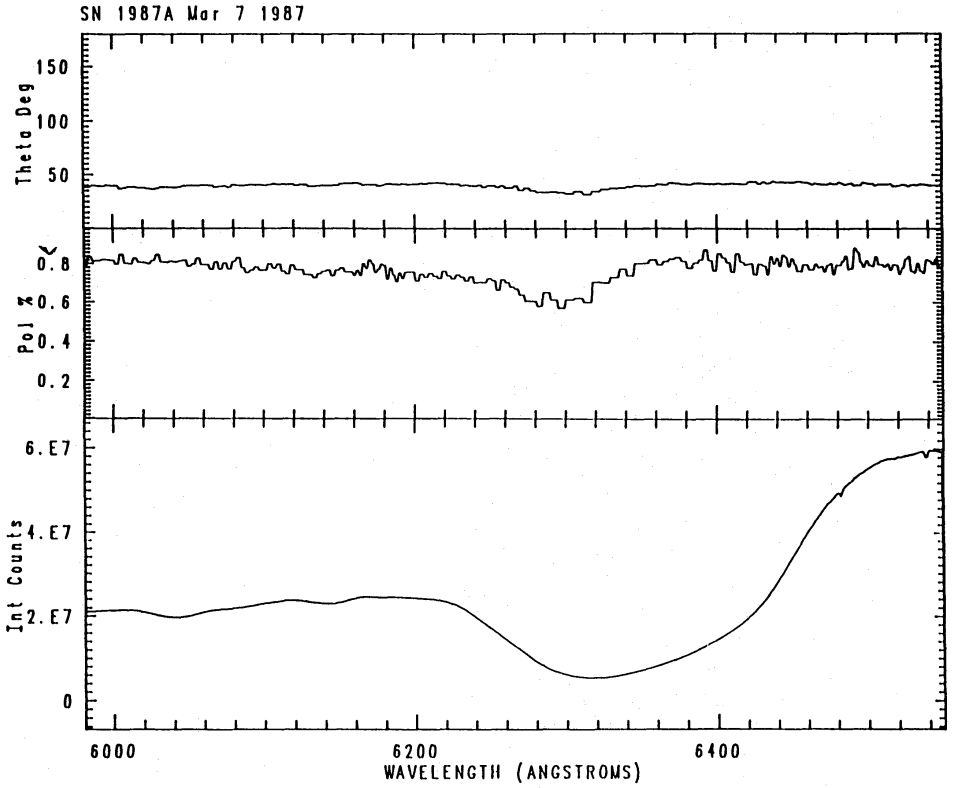

Figure 3. Spectropolarimetry of SN 1987A on March 7 using the GEC CCD as detector at a wavelength centred on the Hα absorption trough.

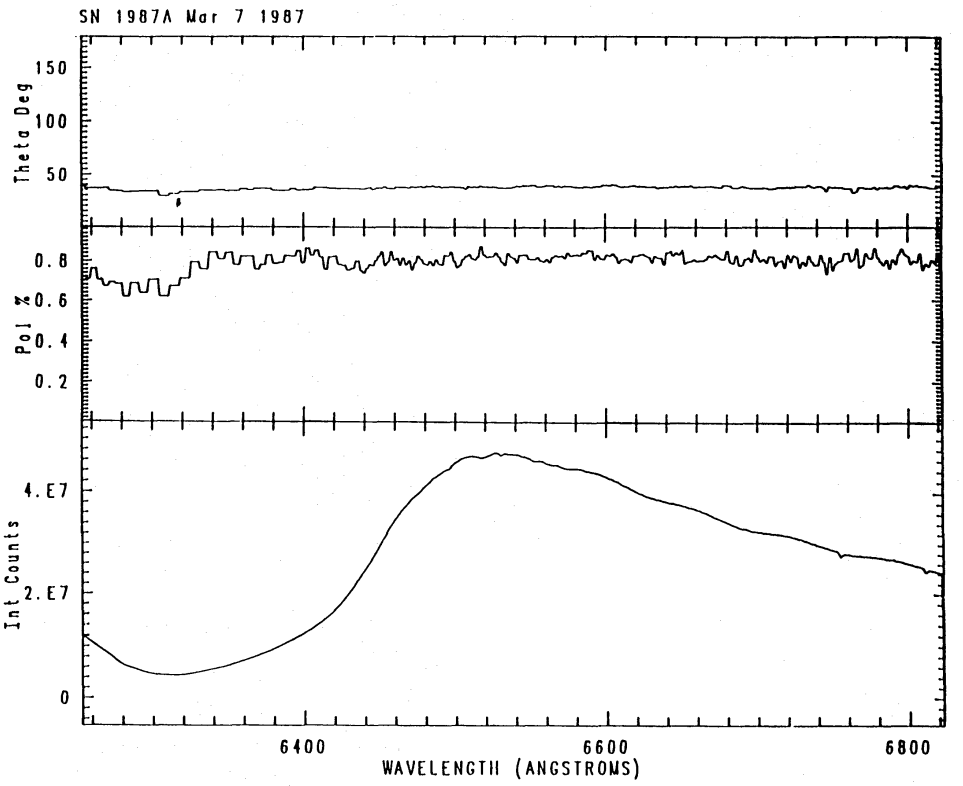

Figure 4. Spectropolarimetry of SN 1987A on March 7 using the GEC CCD as detector at a wavelength centred on the Hα emission peak.

end of this spectrum overlaps with the red end of the spectrum in Fig. 6. The polarizations and position angles measured in this overlap region are similar (note the different plot scales). The polarization through this region is low (<0.2 per cent), except through the Na I *D* lines at 5800 Å, where it rises to a level of ~1 per cent. The ragged appearance of the position angle is again due to the switch from 0° to 180°. To some extent this is caused by the interstellar polarization (see Section 6). The Ca II triplet is extremely strongly polarized at the wavelength of the absorption trough (3.5 per cent), and there is polarization over the rest of the line. The position angle decreases to a flat minimum after dropping from a higher value at the sharp polarization peak and it rises again to higher values at the red end of the emission line.

The June 28 observations (Fig. 9) were taken under very poor observing conditions. It is possible that there are unknown systematic effects in these measurements. Nevertheless, they show that the high levels of polarization through the Hα profile recorded four weeks beforehand have dropped dramatically. For the first time we took circular polarization measurements. Again, our S/N ratios were not very high; nevertheless it was clear that there were no strong features in the circular polarization spectrum.

Figs 10 to 13 show the polarizations taken in the blue part of the spectrum using the RCA CCD as a detector between July 3 and 5. The response of the RCA CCD below 4000 Å is poor and by the time of these observations SN 1987A had become faint in the blue part of the spectrum. These two factors resulted in a spectrum with almost no information shortward of 4000 Å. A strong and broad polarization feature is visible at 4220 Å. The continuum polarization has risen to ~1 per cent at this epoch. A series of three broad polarization features is visible between 4800 and 5200 Å (Figs 11 and 12). These also show small variations in their position angles. The Na I *D* lines (Fig. 13) at 5800 Å are again visible in the polarization spectrum as a double-peaked feature.

Our last set of observations was made on July 8. Fig. 14 again shows the region around Hα. In

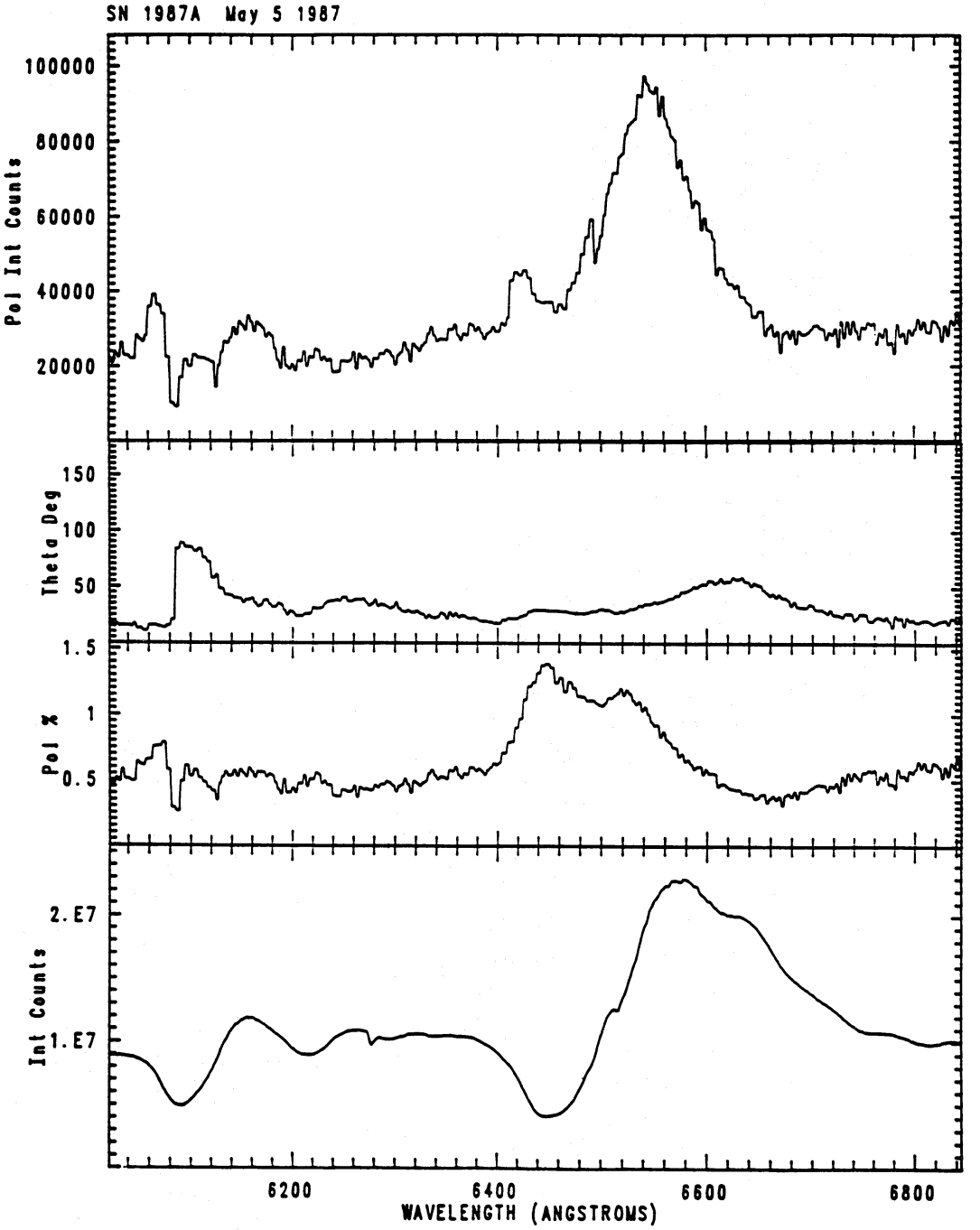

Figure 5. Spectropolarimetry of SN 1987A on May 5 using the GEC CCD as detector at a wavelength centred on Hα.

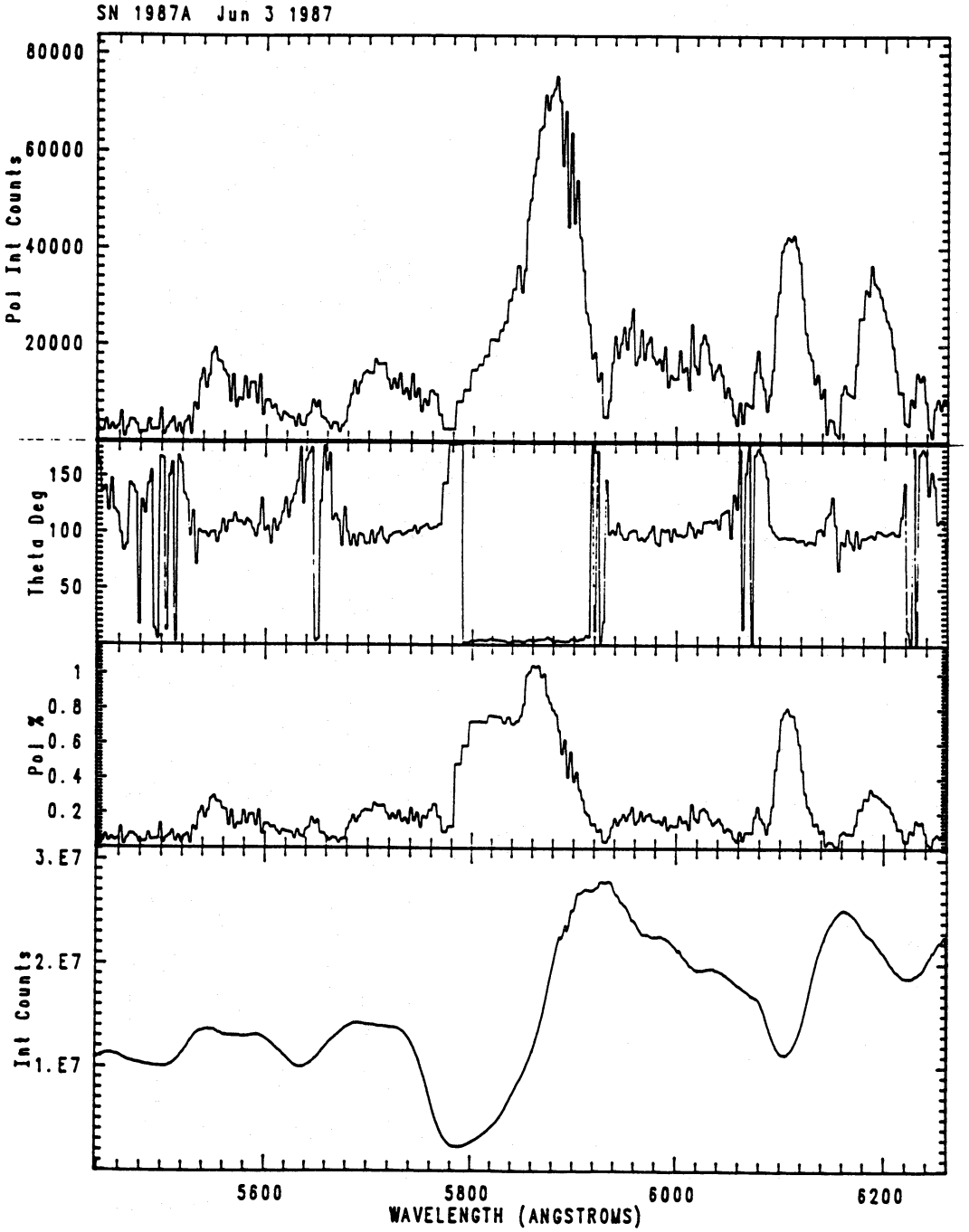

Figure 6. Spectropolarimetry of SN 1987A on June 3 using the GEC CCD as detector at a wavelength centred on 5800 Å.

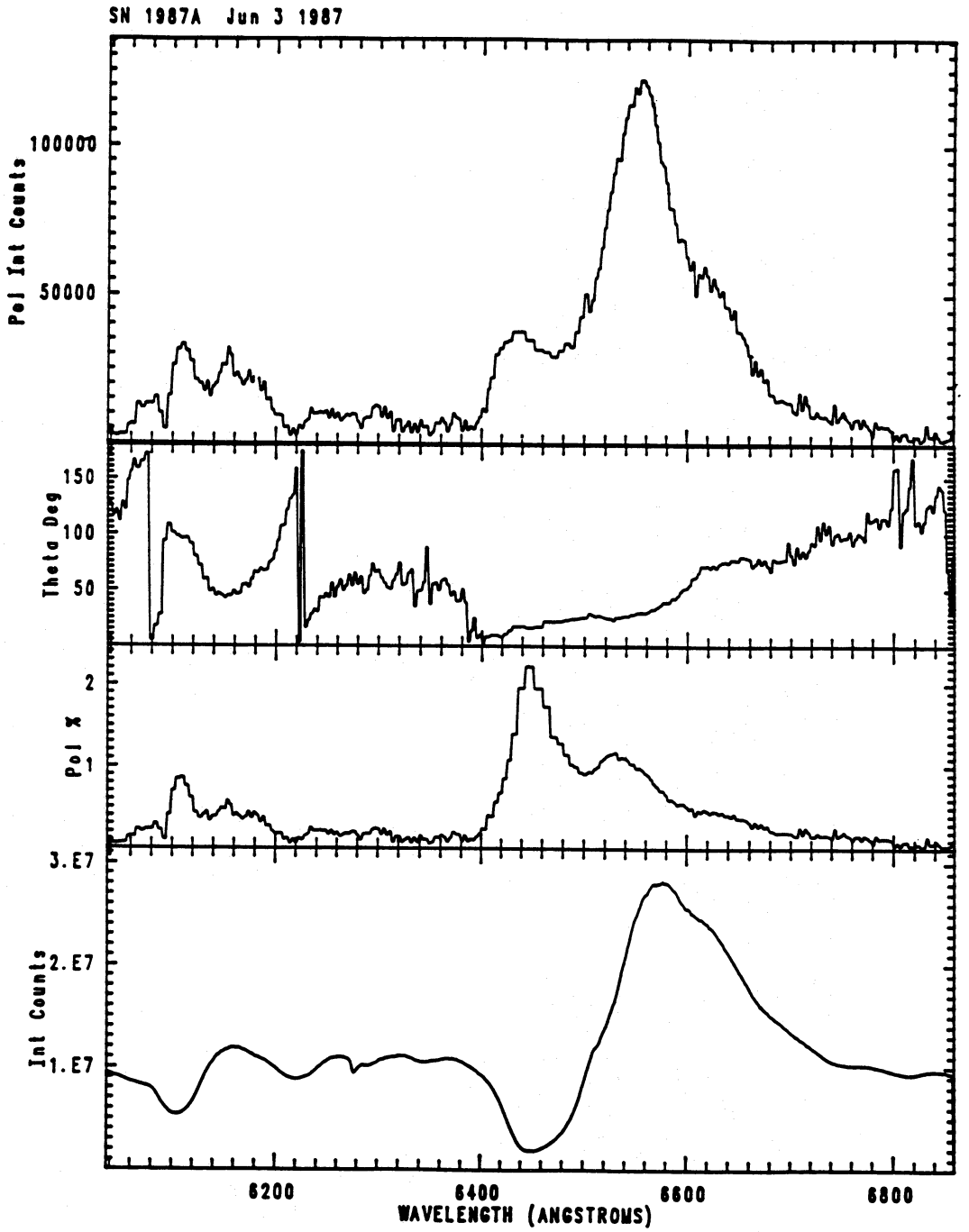

Figure 7. Spectropolarimetry of SN 1987A on June 3 using the GEC CCD as detector at a wavelength centred on Hα.

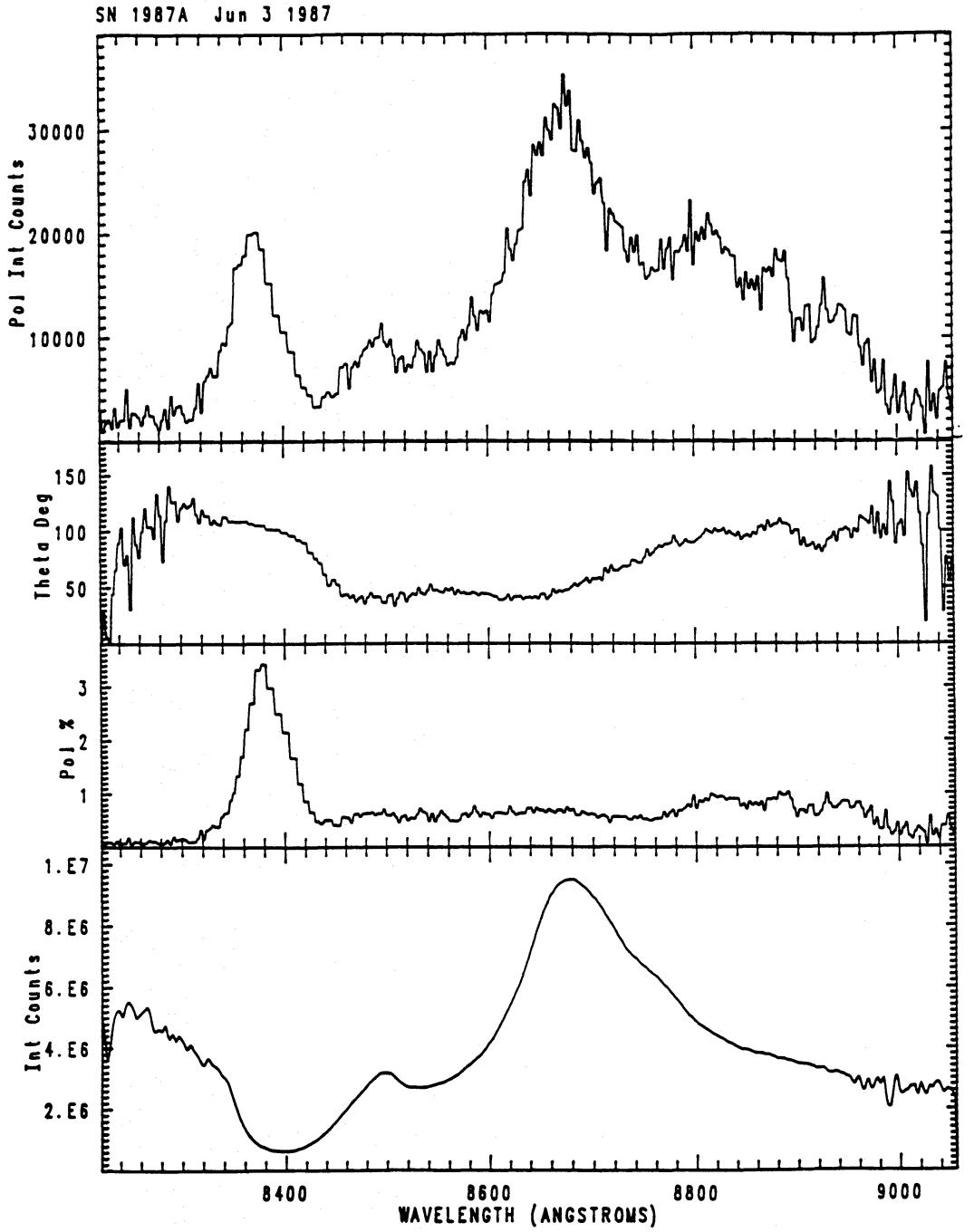

Figure 8. Spectropolarimetry of SN 1987A on June 3 using the GEC CCD as detector at a wavelength centred on the Ca II triplet.

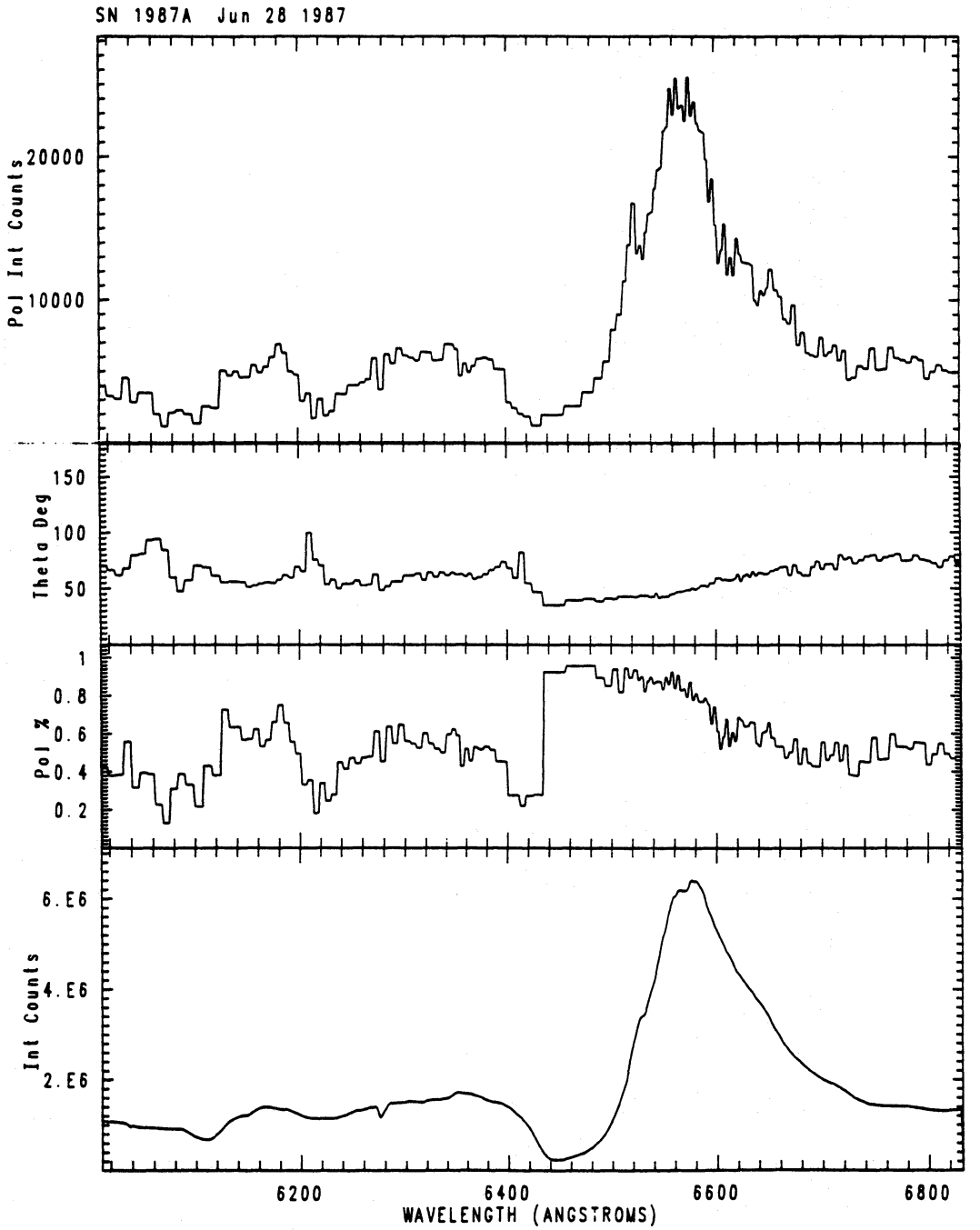

Figure 9. Spectropolarimetry of SN 1987A on June 28 using the GEC CCD as detector at a wavelength centred on Hα.

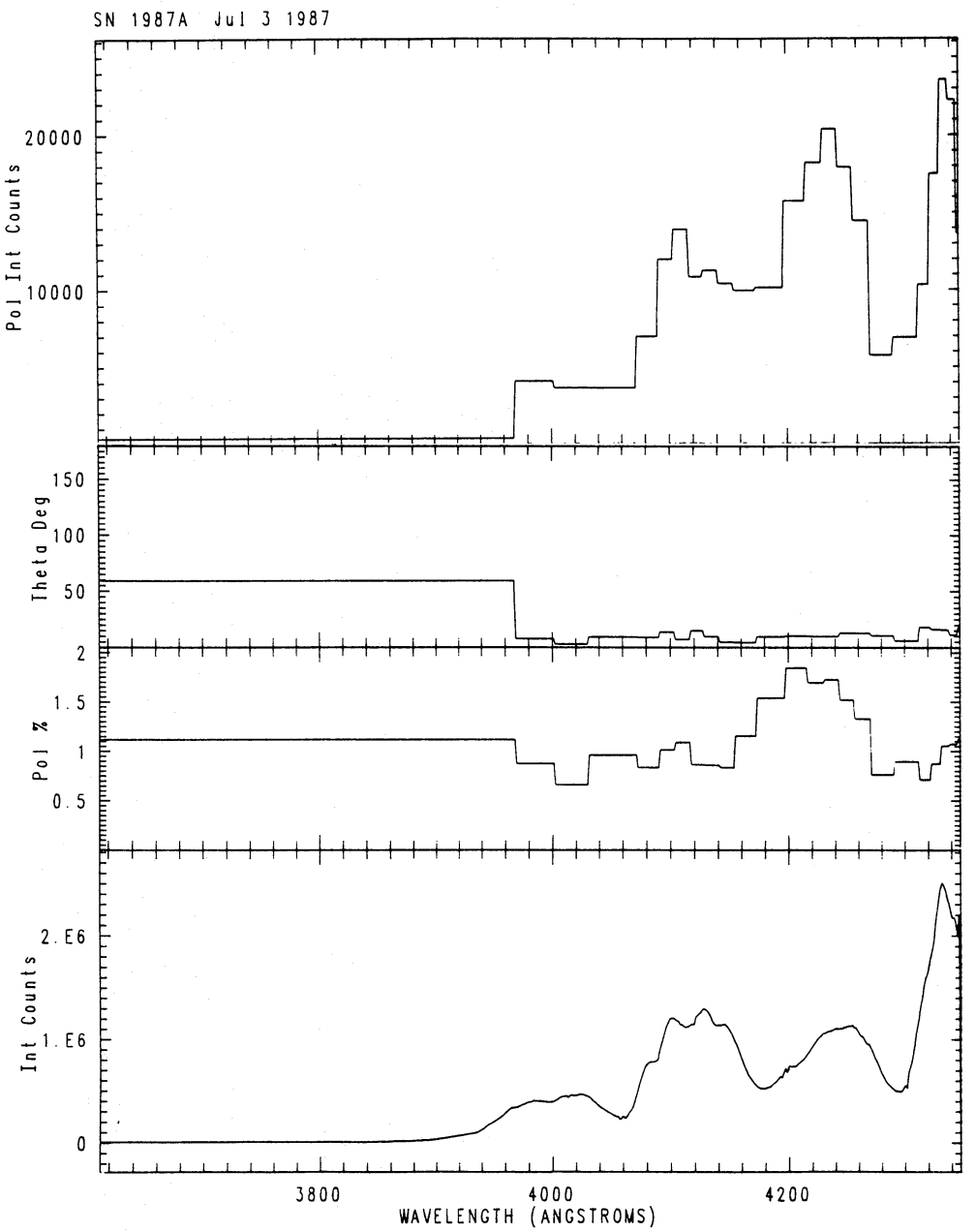

Figure 10. Spectropolarimetry of SN 1987A on July 3 using the RCA CCD as detector at a wavelength centred on 4000 Å.

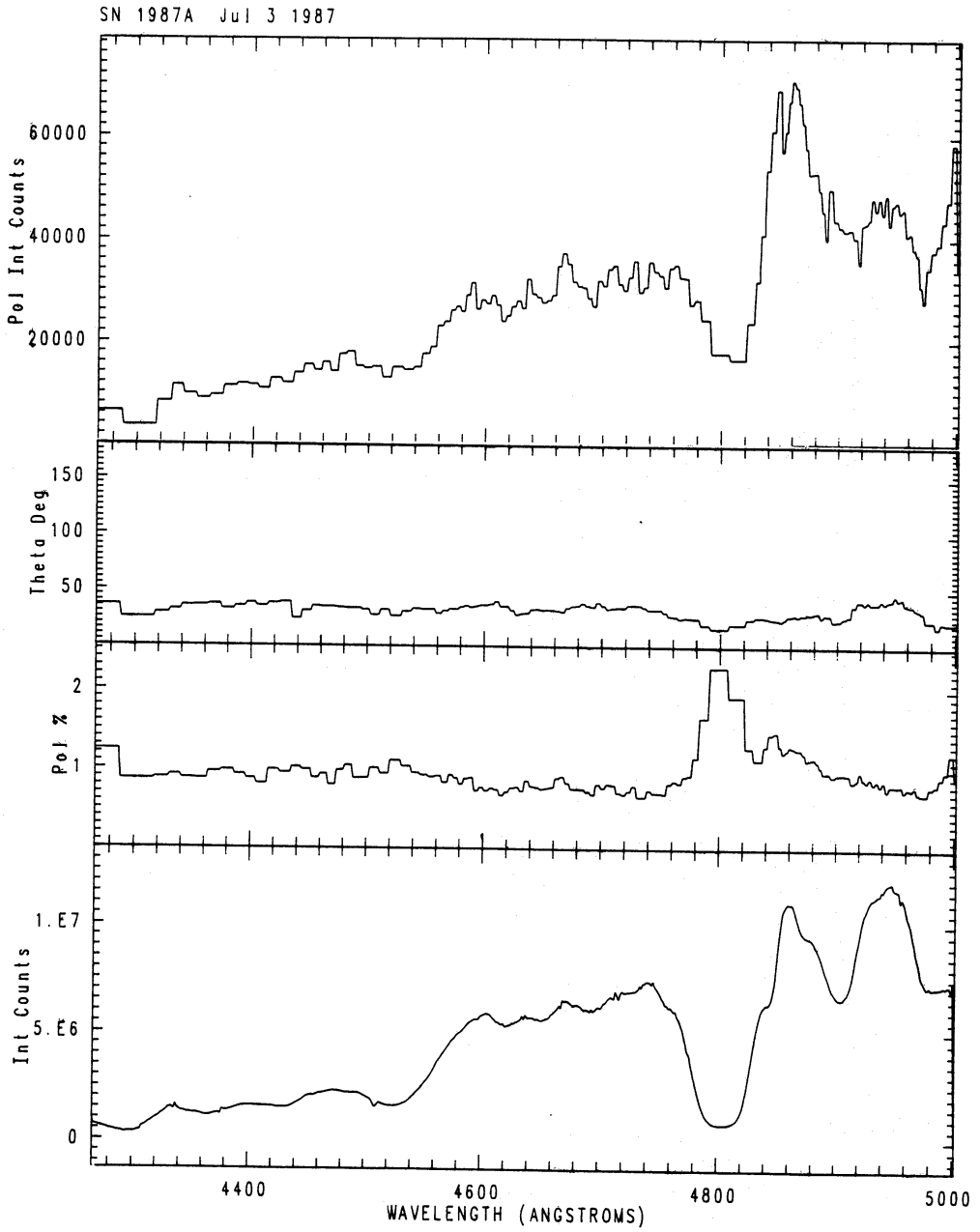

Figure 11. Spectropolarimetry of SN 1987A on July 3 using the RCA CCD as detector at a wavelength centred on 4600 Å.

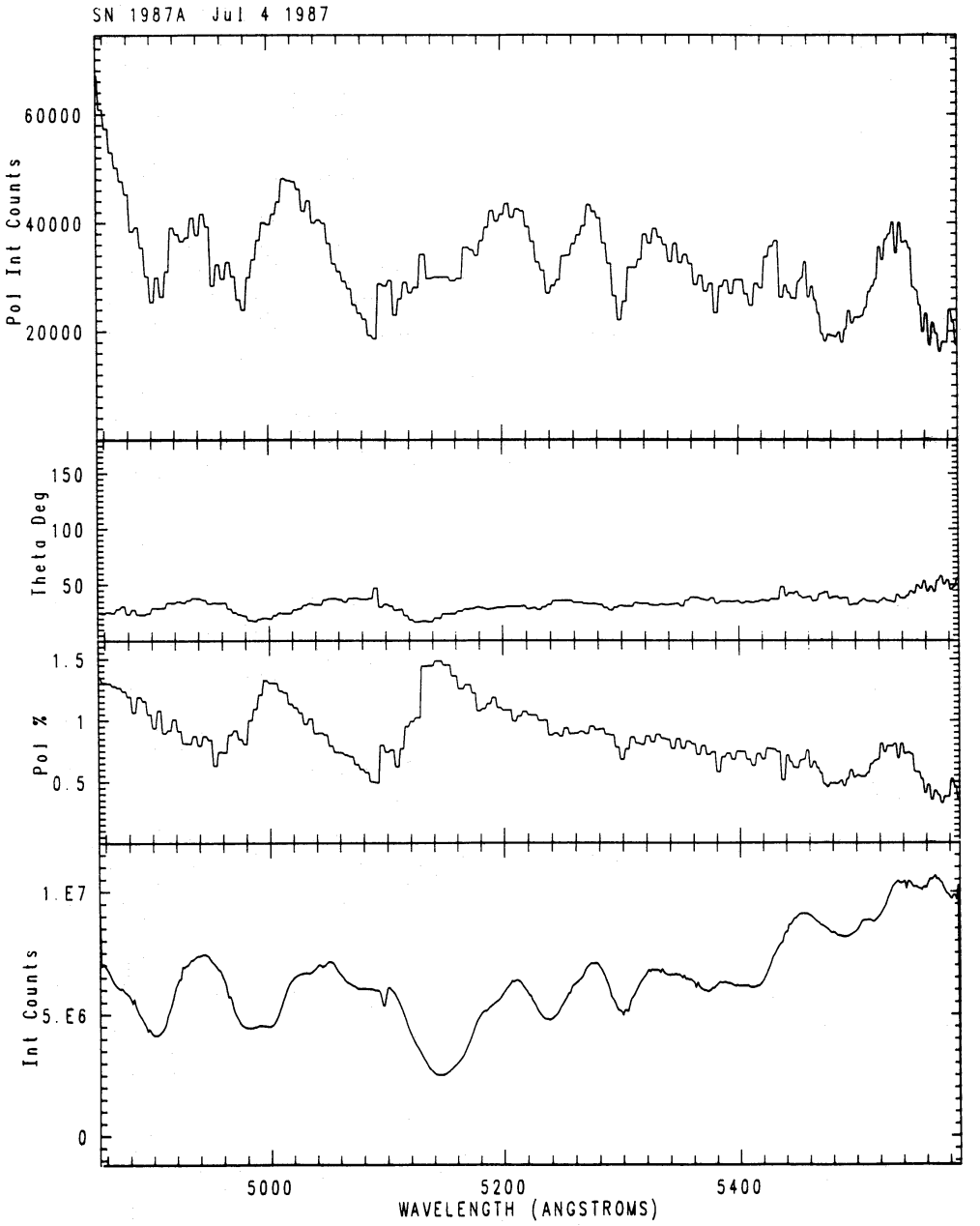

Figure 12. Spectropolarimetry of SN 1987A on July 4 using the RCA CCD as detector at a wavelength centred on 5200 Å.

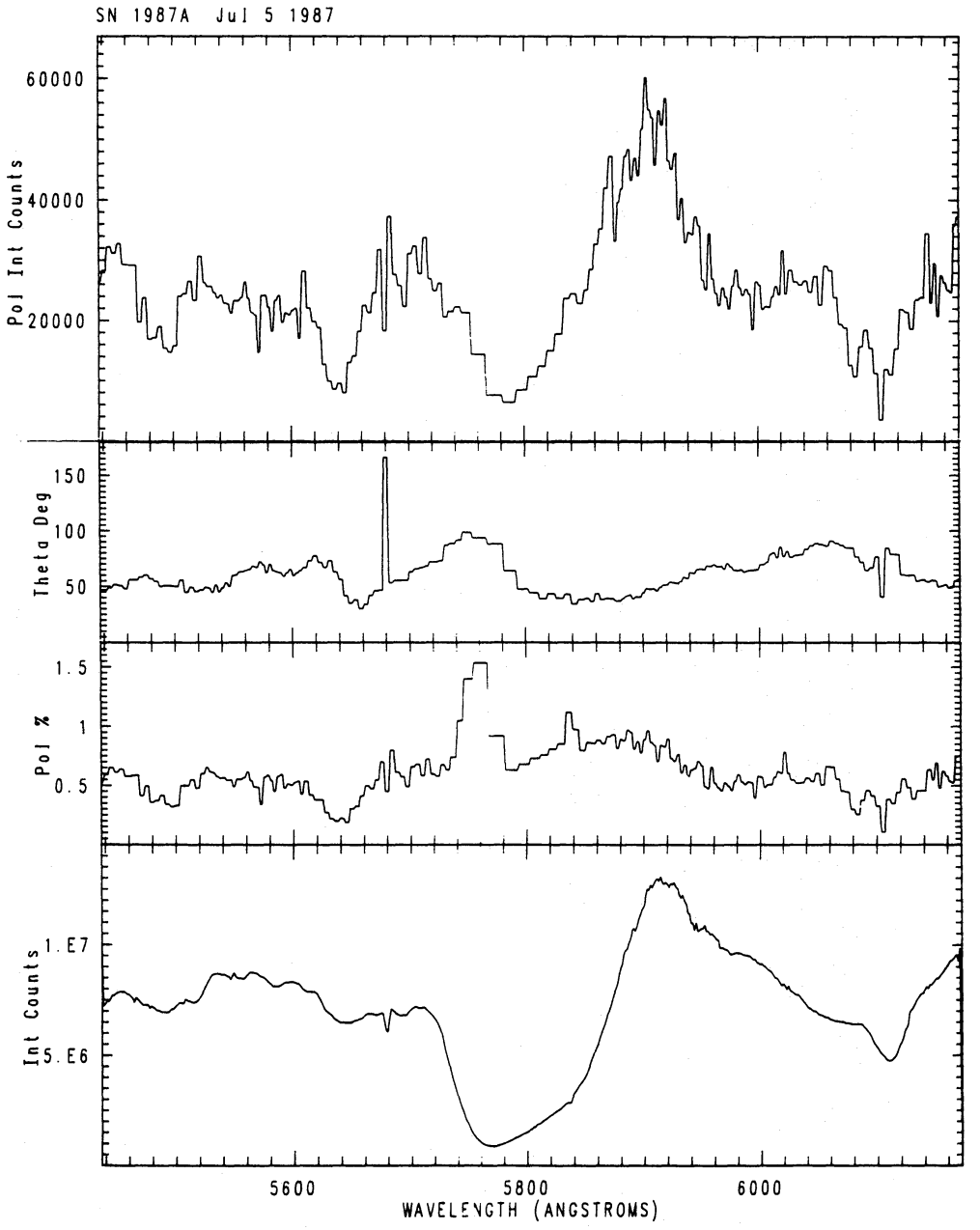

Figure 13. Spectropolarimetry of SN 1987A on July 5 using the RCA CCD as detector at a wavelength centred on 5800 Å.

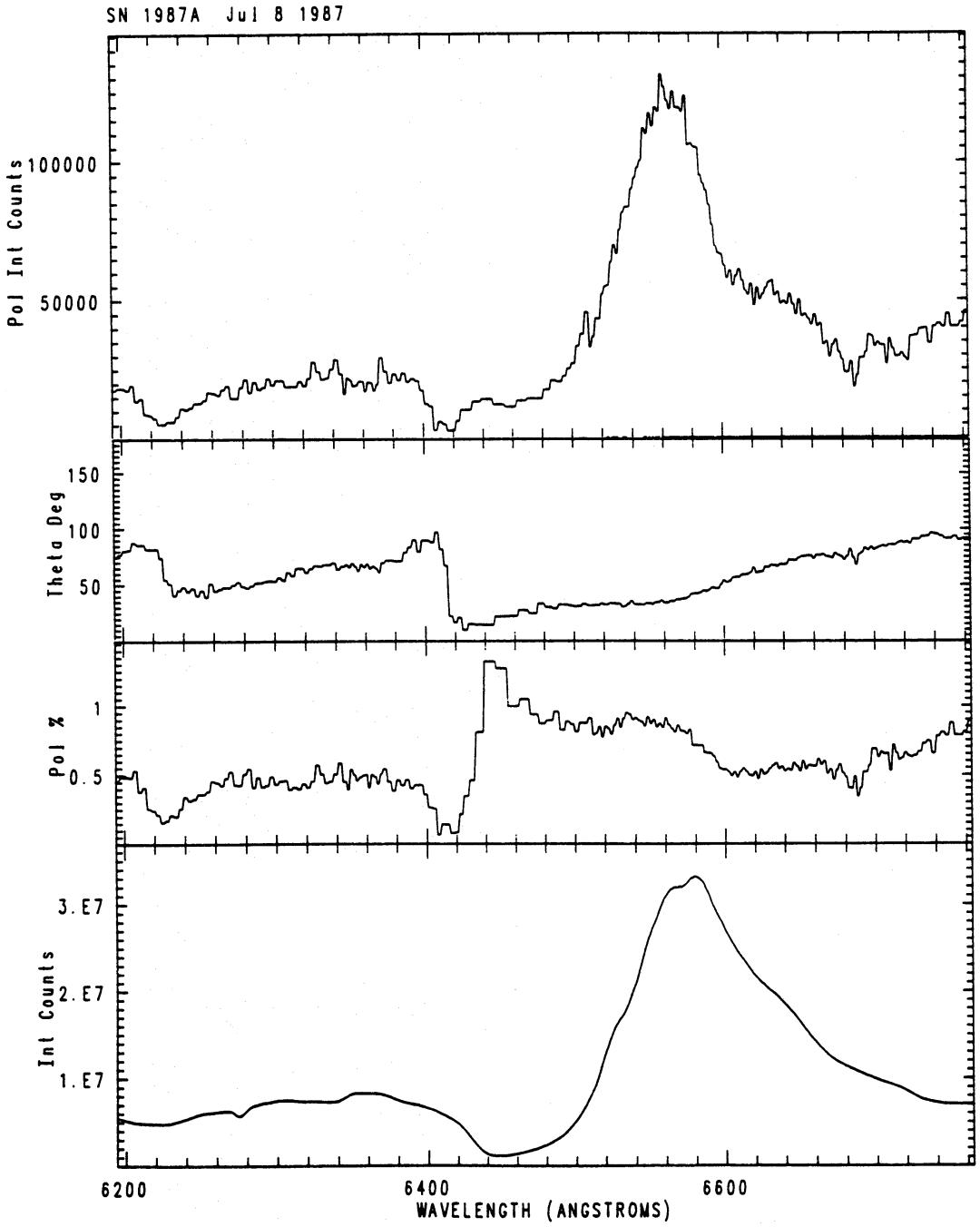

Figure 14. Spectropolarimetry of SN 1987A on July 8 using the GEC CCD as detector at a wavelength centred on Hα.

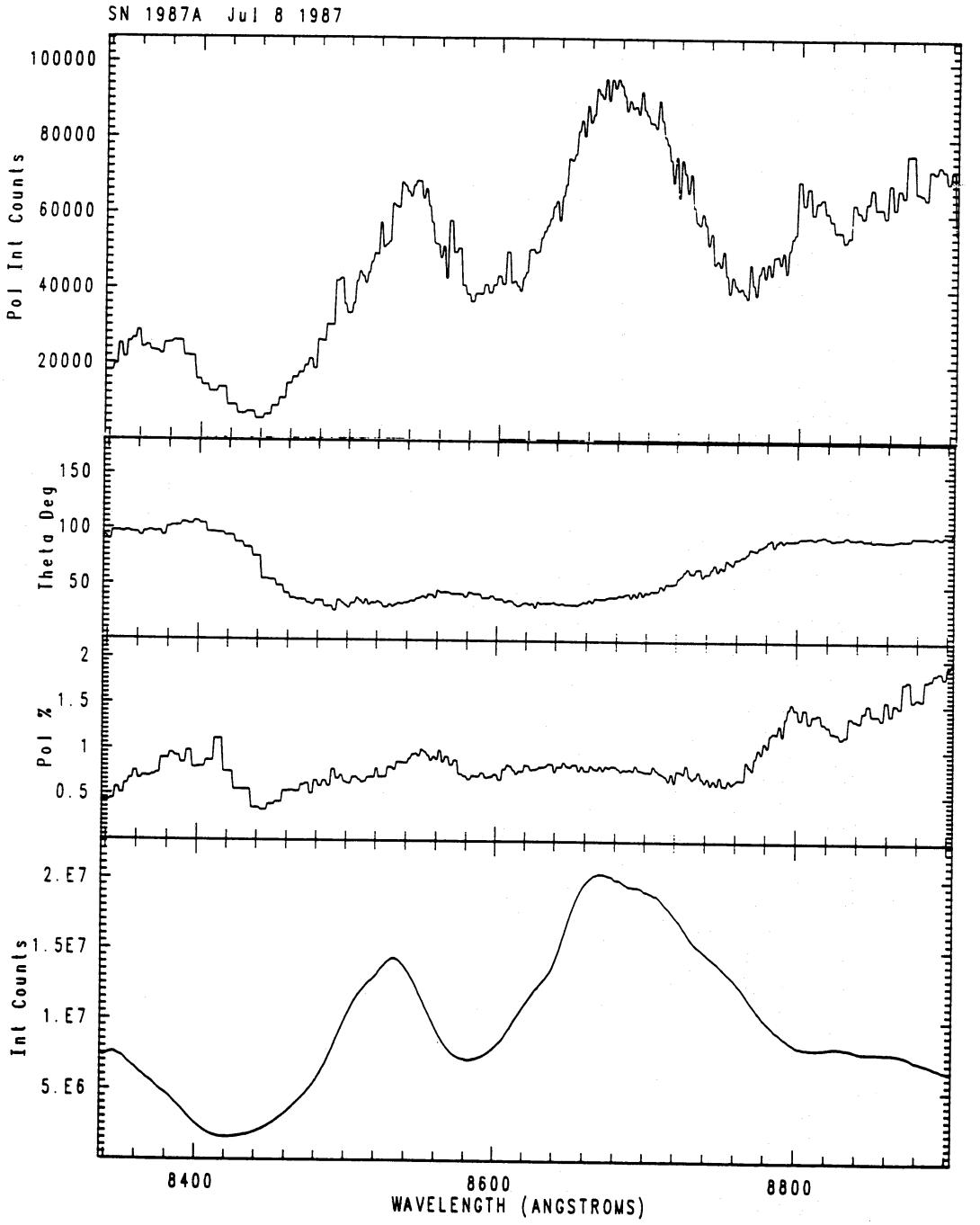

Figure 15. Spectropolarimetry of SN 1987A on July 8 using the GEC CCD as detector at a wavelength centred on the Ca II triplet.

agreement with the blue data a few nights previously, the continuum level is still at ~0.5 per cent. The decreasing trend in height of the polarization peak seen on July 28 in poor conditions is also confirmed. The very strong peak in the Ca II triplet is entirely absent (Fig. 15), although the position-angle variation is similar to that seen on June 3. Again we have circular polarization measurements, this time with better S/N ratios. There may be significant circular polarization at a level $\lesssim$0.2 per cent, especially at the Ca II triplet. However, it is notable that this modulation is strongly correlated with *linearly polarized flux* (top panel in Fig. 15) and because the Pockels cell modulator used in the spectropolarimeter can be adjusted to a quarter-wave retardance only at

wavelengths shorter than 7500 Å this may be caused by linear-to-circular conversion inside the instrument. On the other hand it may also be real. The instrumental effects are under investigation and if the circular polarization is proved to be significant it will be the subject of a subsequent discussion.

6 The interstellar component

As is evident from Figs 2 to 15, the polarization of SN 1987A has evolved with time and depends strongly on wavelength. Some of the polarization is therefore intrinsic (Section 7.3). However, intervening dust in both our Galaxy and within the LMC will further polarize the light from SN 1987A. We attempt below to determine a value for this component in the polarization.

Unfortunately, no polarization measurements exist of the proposed progenitor, Sanduleak −69°202, before the outburst. In addition, the polarization of a nearby 10th magnitude star measured by Barrett (1987a) must also be viewed with caution in the light of his later report that this had varied (Barrett 1987b). However, the polarization both of foreground stars in the direction of the LMC and of stars in the LMC itself has been investigated by Mathewson & Ford (1970) and Schmidt (1976).

We first consider the foreground component due to our Galaxy. Mathewson & Ford (1970) concluded that the Galactic polarization is relatively small and constant in the direction of the LMC and determined a value of 0.3 per cent at a position angle of 30°. Schmidt (1976) went a step further and divided the LMC into five fields to allow a more detailed investigation into the variation of the polarization in each direction. SN 1987A falls in his field IX, for which he determined a foreground polarization of 0.40±0.11 per cent at a position angle of 20°. These two determinations are in good agreement.

The polarization caused by dust in the LMC itself is more problematic because it is not clear how far within the LMC the supernova is embedded. The star closest to the supernova in the Mathewson & Ford investigation is Sanduleak −69°209A, 2 arcmin East and 4 arcmin North with a polarization of 0.95±0.13 per cent at 19°±4°. Correcting this value using the Schmidt (1976) value for the foreground gives 0.55 per cent at 18°. Within ~15 arcmin there are 10 other stars in their catalogue (listed here in Table 2) with corrected polarizations varying between 0.09 and 2.43 per cent. The corrected polarizations are shown in Fig. 16. Therefore, from the polarizations of the surrounding stars the polarization caused by dust in the LMC could be anything up to 2.5 per cent or even more. An upper limit is, however, set up by the extinction. Danziger *et al.* (1987) determined a visual absorption A_V of 0.66±0.2 using the Hα/Hβ decrement of the H II region surrounding the supernova. West *et al.* (1987) determined A_V=0.6 from pre-outburst *UBVRI*

Table 2. List of the stars with polarizations measured by Mathewson & Ford (1970) near SN 1987A. The polarizations are corrected for galactic foreground polarization using the value from Schmidt (1976).

Star	Offsets (arcmin)			Observed Polarizations		Corrected	
	$\Delta\alpha$	$\Delta\delta$	Total	P (%)	θ (deg)	P (%)	θ (deg)
−69°231	−11	5	12	0.89±0.16	56±5	0.86	69
−69°223	−8	−4	9	1.59±0.09	99±2	1.97	101
−69°219	−6	−7	9	2.19±0.14	81±2	2.43	85
−69°216	−6	7	9	0.49±0.07	21±4	0.09	25
−69°215	−5	−9	10	1.13±0.15	90±4	1.46	95
−69°211	−4	8	9	0.63±0.08	25±5	0.25	33
−69°209A	−2	−4	4	0.95±0.13	19±4	0.55	18
−69°209	−2	15	15	1.00±0.40	14±18	0.61	10
−69°204	0	11	11	0.50±0.20	14±18	0.14	175
−69°182	13	7	15	0.51±0.21	46±11	0.41	71
−69°181	16	−3	16	0.41±0.22	45±14	0.34	77

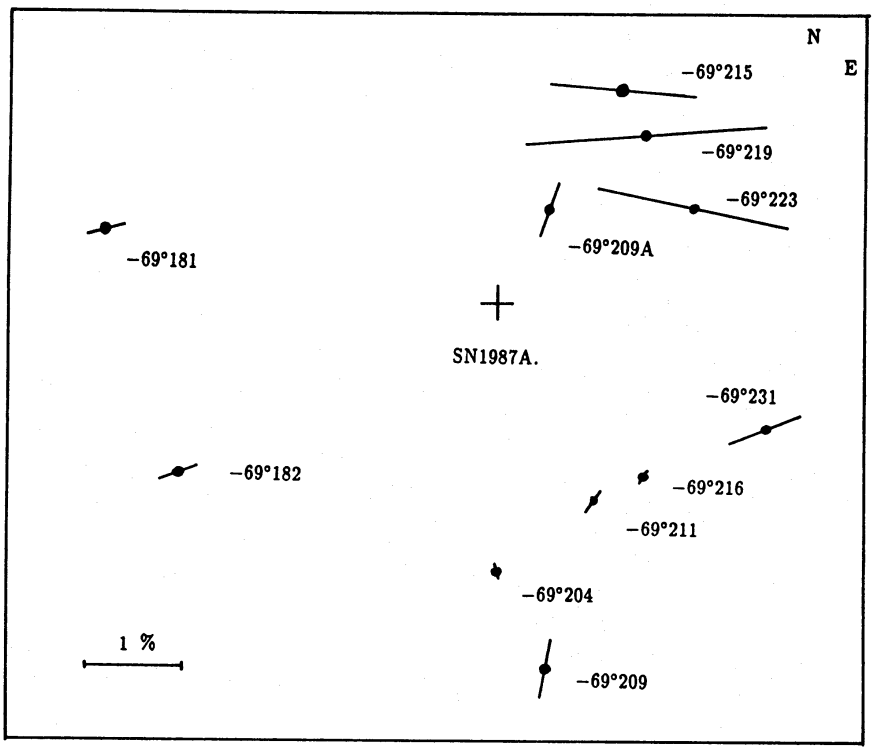

Figure 16. The stars with measured polarizations within ~15 arcmin of SN 1987A from Mathewson & Ford (1970). The galactic foreground polarization determined by Schmidt (1976) has been subtracted. Note the region of higher LMC polarization in the north-east corner.

photographic plates of the region. Using the standard value for the ratio of total to selective extinction $R=A_V/E(B-V)=3.3\pm0.3$ (Martin 1978) then $E(B-V)=0.2\pm0.05$. At a maximum efficiency of polarization by the grains the polarization will be 1.8 per cent for $E(B-V)=0.2$ using the standard relation of P_{max} with $E(B-V)$ of 9 per cent mag^{-1}. This value is an upper limit since the polarization efficiency will generally be lower.

Returning to Table 2, there are two stars which exceed this limit (−69°223 and −69°129). As seen in Fig. 16, these two stars lie close to one another and their polarizations have similar position angles. The third most strongly polarized star, −69°215, also lies nearby and has a similar position angle to the other two. These stars (and −69°231) in the north-east corner of Fig. 16 lie behind a greater amount of polarizing dust. The amount of dust in the direction of the other stars is less. If these other stars are located at a range of depths in the LMC (which is possible) then it is likely that the amount of polarizing dust in the direction of SN 1987A and all the way through the LMC is also small. The mean polarization intrinsic to the LMC for these stars is ~0.3 per cent at ~30° (non-vector sum). Until a more detailed investigation of the stars surrounding SN 1987A is carried out, this is probably the best estimate we can make for the intrinsic LMC polarization. The total polarization caused by dust both in the galaxy and LMC in this direction is therefore calculated to be ~0.7 per cent at ~25°.

Because we regard the determinations for polarizations of the interstellar component from the LMC itself to be uncertain at present, we have presented our data uncorrected for any interstellar polarization in Figs 2 to 15.

Although the data are probably consistent with the flat polarization level of 0.8 per cent at 35°–40° shown by the supernova in the early stages being entirely interstellar in origin, the wavelength-dependence of the broad-band polarizations reported by Cropper *et al.* (1987) and Bailey, Ogura & Sato (1987) (which bracket the March 7 observation) does not conform to the

standard empirical law determined by Serkowski (1974). The measured infrared polarizations are well above the expected contribution, indicating that some of the polarization is intrinsic, at least in the infrared.

7 Discussion

7.1 WHY SUPERNOVAE MAY BE POLARIZED

In a supernova, the spectral lines are caused by resonance scattering and the continuum by electron scattering of photons in an atmosphere above a photosphere emitting a thermal continuum (Branch 1980). Both these forms of scattering will introduce polarization in an unpolarized incident beam, or will modify the polarization state of an already polarized beam.

In a spherically symmetric explosion, the polarizations generated by these scattering mechanisms will, when integrated over the scattering atmosphere, cancel and hence be zero. However, if the supernova envelope is not spherically symmetric a residual polarization will be observed. Electron scattering in an asymmetric atmosphere will cause a continuum polarization, independent of wavelength, while resonance scattering will introduce wavelength-dependent polarization associated with the line features in the spectrum.

7.2 WHY POLARIMETRY OF SUPERNOVAE IS IMPORTANT

As discussed above, the presence of polarization in the light from a supernova is an indication that the scattering atmosphere departs from spherical symmetry. Spectropolarimetry provides more detailed information in that it allows the asymmetries to be investigated at the optical depths at which the lines are formed. This information is available well before the remnant is resolved and at a time before other complicating factors (for example, the inhomogeneity of the interstellar medium in the vicinity of the supernova) may have become dominant. It is important for the following reasons:

(i) It provides insight into the kinematics of the supernova explosion;

(ii) It provides additional constraints on the physical conditions of the scattering atmosphere which are in addition to, and different from, those provided by the line profile shapes;

(iii) Distances to supernovae derived by using the Baade method are valuable in setting up the extragalactic distance scale because they are independent of other calibrations. However, this method assumes spherical expansion of the atmosphere. If the expansion is asymmetric this has serious consequences for such distance determinators [as discussed by McCall (1984)];

(iv) It may determine whether binary companions are present.

7.3 INTERPRETATION

The first steps can be taken using only the simplest assumptions:

(i) The time variability of the polarization, the existence of strong features across the lines in the polarization spectrum and the wavelength-dependence of the broad-band polarizations all indicate that there is considerable intrinsic polarization. Therefore *some asphericity is present* in the scattering atmosphere.

(ii) When the spectra are plotted in the Stokes-parameter QU plane (Fig. 17a–h), the loci traced out are loops, rather than lines. Therefore *the symmetry axis of the aspheric region is different at different wavelengths*.

7.3.1 Complicating effects

From here on the interpretation becomes more problematic. This initially arises because of the complication of dust. Vectorial subtraction of the interstellar component from the observed polarization (see Martin 1978) modifies the polarization spectrum considerably. Dips can become humps and *vice versa*. For example, the March 7 data show a small dip in the polarization and position angle at ~6300 Å. If we subtract 0.7 per cent at 25°, which we proposed as the most likely value for the interstellar component, the mean level of the polarization outside of the dip drops to 0.28 per cent at 65°. The dip in the polarization becomes relatively deeper as the polarization drops to only 0.2 per cent. The hint of a dip of the position angle (over the same region) becomes a more prominent bump, with the position angle rising to 90°. However, if a different, but quite plausible, value is adopted for the interstellar component, for example the value 0.97 per cent at 37° given by Barrett (1987a) and used by Schwarz & Mundt (1987), the polarization dip becomes a polarization bump. Any value of interstellar polarization (in per cent) with $\cos 2\theta \gtrsim 0.7/P$ (where P is the polarization and θ its position angle) will have the effect of turning the dip into a bump. This explains the conclusion of Schwarz & Mundt (1987) that the polarization in the absorption

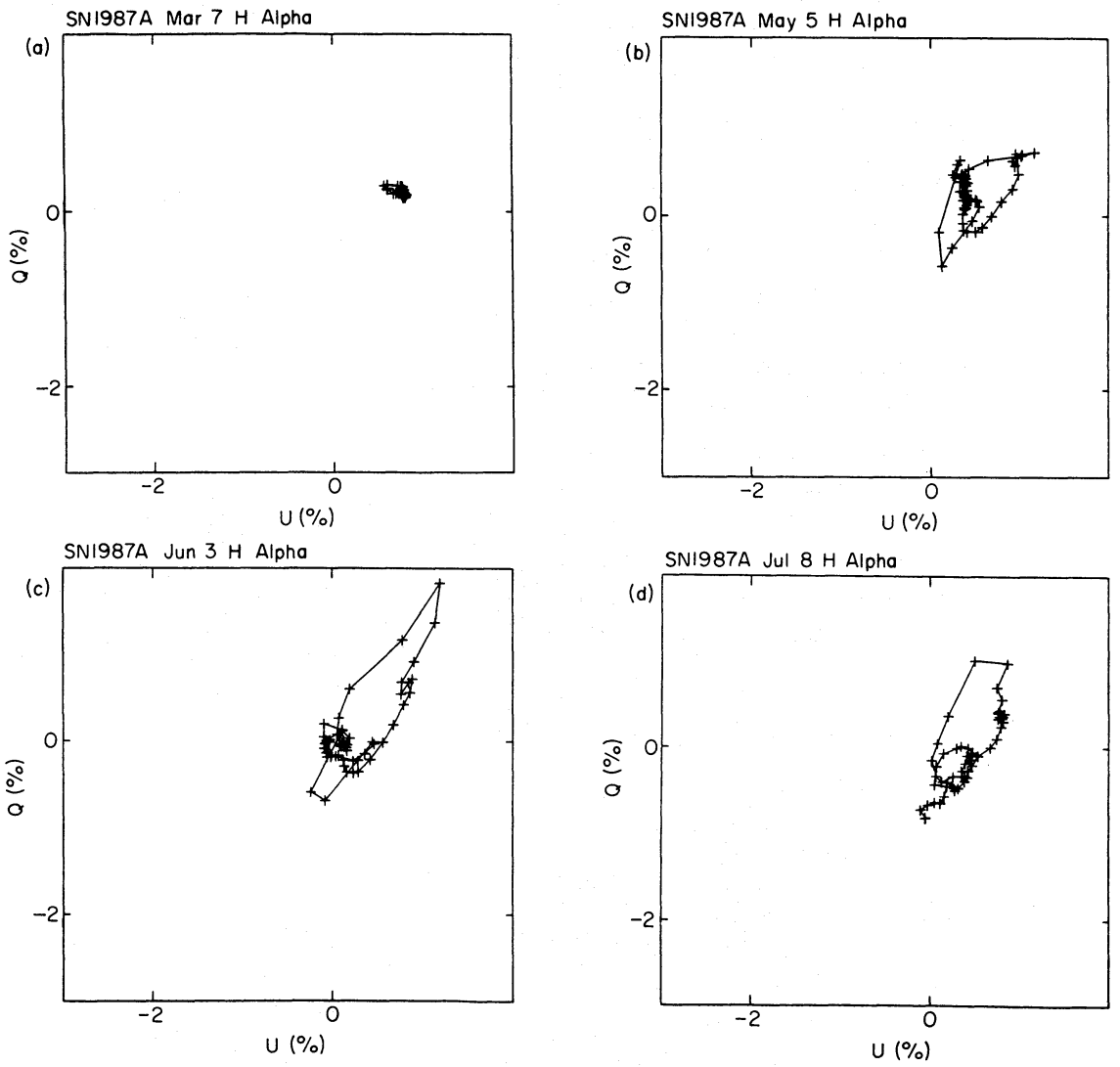

Figure 17. The wavelength-dependence of the spectral lines in the Stokes-parameter QU plane: (a) March 7, Hα; (b) May 5, Hα; (c) June 3, Hα; (d) July 8, Hα; (e) June 3, Ca II triplet; (f) July 8, Ca II triplet; (g) June 3, 5800 Å region and (h) all the above superimposed.

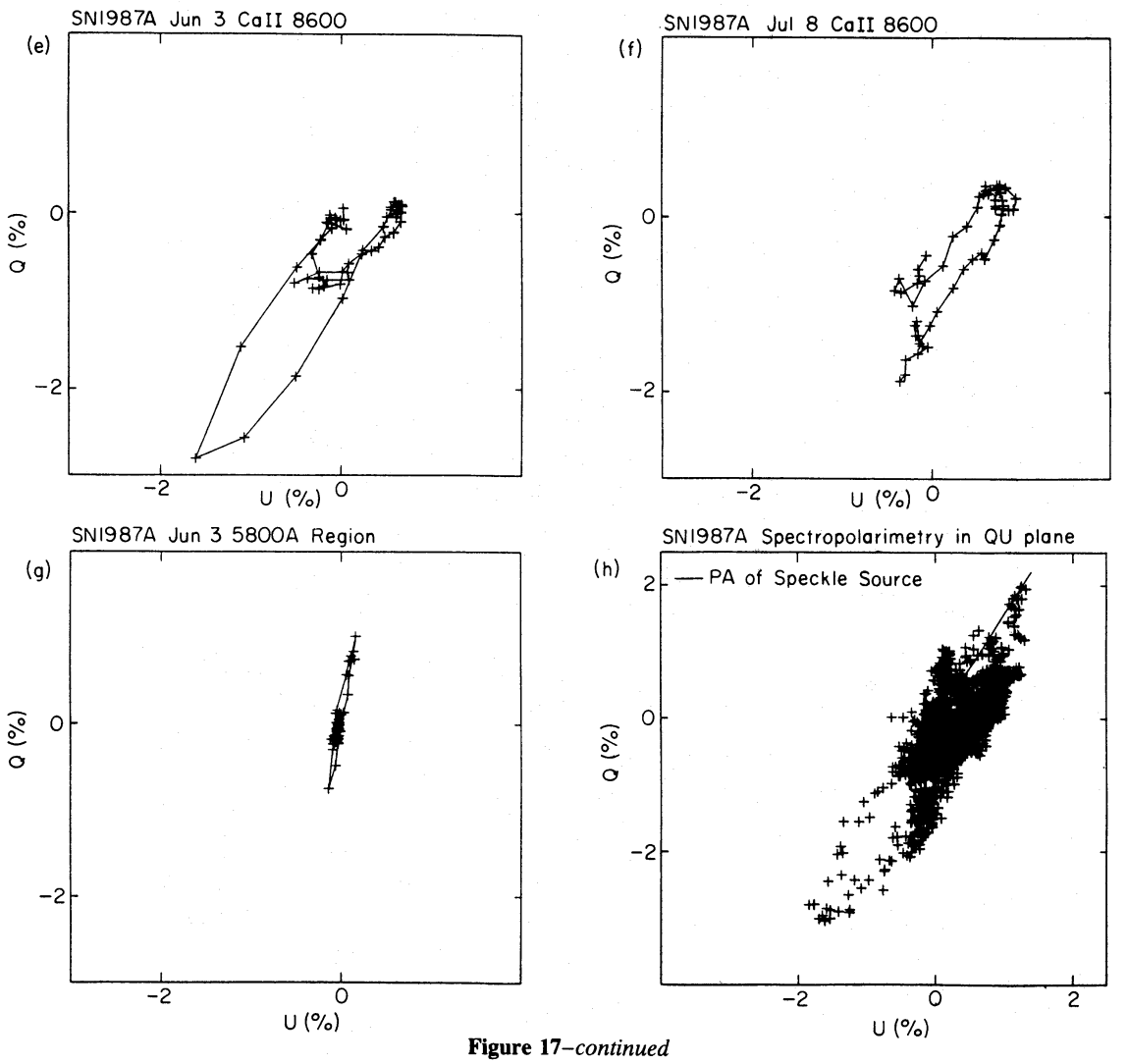

Figure 17–*continued*

line is greater than that in the continuum. (Note, however, that the ISP point denoting the interstellar polarization in their fig. 1 is incorrectly positioned.)

Similar comments apply to the profiles measured at later epochs. The double-peaked profile between 6400 and 6600 Å in the May 5 observations is broader and lower and extends out to 6700 Å when corrected for interstellar polarization. By June 3 the broad long-wavelength peak has almost disappeared and the main features are the remaining peak at 6450 Å and a broad depression from 6500 to 6650 Å. Even the remaining peak has disappeared by the July 8 observation and only the broad depression is left.

As discussed in Section 7.1, there are two sources of polarization – electron scattering and resonance scattering. The geometrical shapes of the atmospheres at the optical depth where each effect becomes most important at a particular wavelength may be completely different. Now, the electron scattering will *also* contribute to the observed polarization through the line in a manner similar to that contributed by the interstellar polarization. In addition, the contribution from the electron scattering will change as the scattering atmosphere evolves. Therefore, in order to study the resonance scattering through the line, the polarizations should perhaps be shown relative to the polarization at some wavelength outside the line which may be different as the supernova evolves. Alternatively, they may be plotted on the Stokes-parameter QU plane as shown in Fig. 17.

In order to progress further, detailed modelling is required.

7.3.2 *Polarization models*

Probably because of their complexity and the paucity of spectropolarimetric observations of supernovae [only one set exists and the S/N ratio of these was sufficient only to set upper limits to the variation of polarization through the lines – see McCall *et al.* (1984)], there has been little theoretical work on the polarization of supernovae. Shapiro & Sutherland (1982) have determined the linear polarization induced by an elliptical scattering envelope. Although the effects of resonance scattering are included, they treat only the case for the transition $J=0$ to $J=1$ in which case the resonance scattering phase matrix is similar to that for electron scattering. They do not calculate polarization spectra. However, taking a somewhat simpler approach, McCall (1984) predicted, in the only other theoretical investigation available, that the polarization in both the emission and absorption components of the P Cygni line profiles should exceed that in the continuum if the scattering atmosphere is non-spherical.

The data presented here clearly justify a more detailed treatment in which the polarized radiation transfer is an expanding asymmetric supernova atmosphere is taken into account, so as to predict the polarization spectrum across line profiles. A preliminary study by Jeffery (1987, private communication) shows that it is possible to produce results in qualitative agreement with the effects observed, though it is clear that a detailed model of our observations will require considerable further work.

Of course, a fairly substantial body of theoretical work exists for the calculation of polarization profiles across spectral lines in Be stars [for example Poeckert (1982) and references therein and McKenna (1984)]. However, P Cygni profiles are unusual in Be stars, and they have discs, making the problem fundamentally different from that considered here, although Poeckert & Marlborough (1978) did consider the polarizations produced in Be stars with stellar winds. Poeckert's (1982) fig. 10 shows the predicted intensity and polarization profile of Hα as a function of inclination. At inclinations near 90° the line profile is P Cygni shaped and the calculations predict a peak in the linear polarization at the wavelength of the absorption dip and a broad dip in the polarization at the wavelength of the emission peak. This is similar to our observed profiles (especially on June 3) if our estimate of the interstellar polarization is subtracted from the data.

We believe that the extremely high S/N ratio and detailed structure evident in our data will constrain theoretical models very severely. Sophisticated models will have to be produced in order to account both for the details in each spectrum and their time evolution. The development of these will take some time. We therefore limit ourselves in this paper to the interpretation of our results in terms of the simple existing models referred to above.

7.3.3 *Shapiro & Sutherland's model*

In comparing our data with Shapiro's & Sutherland's (1982) model we confine our attention to the March 7 data when (from the shallowness of the polarization features) the polarization was clearly dominated by the interstellar polarization and that caused by electron scattering. With our adopted interstellar polarization of 0.7 per cent at 25° the intrinsic polarization outside the shallow polarization dip (Figs 3 and 4) is 0.28 per cent. For the pure scattering case and a scattering atmosphere in the shape of an oblate spheroid with axis ratio μ, our data imply $\mu=0.77$, while in the prolate spheroid case, $\mu=0.71$ (their fig. 2). This calculation is sensitive to the value adopted for the interstellar polarization.

7.3.4 *McCall's model*

McCall developed his model (McCall 1984) assuming a scattering atmosphere which is an oblate spheroid. This surrounds an unpolarized continuum source assumed to have the same shape.

These atmospheres project to ellipses with similar axis ratios μ. The polarization is assumed to be produced only in the limb region. The model implicitly assumes that the region in the atmosphere where electron scattering occurs is the same as that where the resonance scattering occurs. It predicts that the polarized emission in the lines will be double peaked, because the excess polarization at the emission peak arises from the addition of polarized radiation from the limb while that at the absorption trough occurs because of the reduction of the unpolarized component from the central zone. Furthermore it predicts that the intrinsic plane of polarization is wavelength-independent.

It is clear from our data that this last prediction is not fulfilled: when the polarizations are plotted in the Stokes-parameter QU plane (Fig. 17a–g), the locus of the polarization as a function of wavelength is a series of loops and not a straight line. Therefore, irrespective of the value chosen for the interstellar polarization (thus redefining a new origin in the plane) the locus never approximates a straight line (radial to the new origin) corresponding to a variable amount of polarization at a constant position angle. However, it is also true that for reasonable values of the interstellar polarization, the polarization profiles are double peaked as predicted, at least on May 5 and June 3 (Fig. 17b, c). We therefore proceed, cautiously, a little further.

From McCall's equation (24) the axis ratio of the projected ellipsoids can be calculated as:

$$\mu=\frac{f(\text{emis})[P_0(\text{line})-P(\text{emis})]-[P(\text{emis})-P(\text{cont})]}{f(\text{emis})[P_0(\text{line})+P(\text{emis})]+[P(\text{emis})-P(\text{cont})]}$$

where f(emis) is the ratio of the P Cygni emission to the continuum, P_0(line) is the intrinsic polarization of the line radiation resonance scattered from any point in the limb, P(emis) is the observed polarization at the wavelength of the P Cygni emission and P(cont) is the observed polarization of the continuum. All of these numbers are observables except for the P_0(line) which has a value between 0 and 1. This is not a vector equation, since it assumes as mentioned above that all the polarizations lie in a straight line in the QU plane as a function of wavelength. Some guess therefore has to be made for the interstellar polarization in order to calculate P(emis) and P(cont) correctly. Adopting our best estimate of 0.7 per cent at 25° for the Hα line we calculate

$$\mu=\frac{2.2[P_0(\text{line})-0.002]-0.0084}{2.2[P_0(\text{line})+0.002]+0.0084}$$

for May 5 and

$$\mu=\frac{2.7[P_0(\text{line})-0.003]-0.0076}{2.7[P_0(\text{line})+0.003]+0.0076}$$

for June 3.

The axis ratio can now be calculated using the correct value for P_0(line). This is complicated by the fact that Hα is a multiplet with seven fine-structure components (neglecting the small Lamb shift) (Condon & Shortley 1964). The E coefficients for the resonance-scattering phase matrix of each of these components can be calculated from their J and ΔJ values and the polarization computed using

$$P_0=\frac{I_l-I_r}{I_l+I_r}$$

(Chandrasekhar 1960). For simplicity we have calculated the relative contribution to P_0(line) from each P_0 by considering the scattering at 90° and weighting the component intensities in the ratios given by Dyson & Meaburn (1971) for LTE and Case B conditions. In LTE, P_0(line)=0.092 and in Case B, P_0(line)=0.093. Scattering at other angles will be lower than this. If we take the

mean [P_0(line)=0.0925] then μ=0.88 on both May 5 and June 3. The axis ratio is therefore unchanged between the two observations and the model predicts a significantly aspherical scattering envelope. This would lead to an overestimate by a factor of $\mu^{-1/2}$=1.07 to the distance determination when the Baade–Wesselink method is used. Branch (1987 – paper presented at ESO SN 1987A Workshop) reported that this method gave a distance of 55±5 kpc, while a recent determination of the distance modulus to the LMC is 18.5 (Feast 1986) or 50 kpc. It is interesting, although barely significant, that the differences between these estimates do differ by about the predicted amount.

The axis ratio μ can also be calculated for the March 7 observations. In this case P(emis) and P(cont) are equal. Using P(emis)=0.8 per cent at 37° and our adopted value for the interstellar polarization, μ=0.93. There is therefore some evidence that the asphericity of the envelope increased at later epochs. Although this conclusion depends on the interstellar polarization adopted, interstellar values rather too large result if this is allowed to be the free parameter and μ is forced to the value of 0.88 observed at later epochs.

7.3.5 Additional comments

As stated at the beginning of Section 7.3, because the loci of the spectra in the Stokes-parameter QU plane are loops rather than lines, the asphericity of the scattering envelope is wavelength-dependent. This does not apply only to the lines themselves. The main loop for the June 3 Hα observations extends in a direction ~35° in the QU plane. On the other hand, that for the June 3 Ca II triplet extends in a direction ~215°, ~180° different. The 5800 Å-region observations on the same date extend in a direction only ~10°. The difference between the orientation of the Hα and Ca II triplet loops indicates that the scattering axes for the two wavelength regions are perpendicular to each other. In terms of the elliptical scattering model of McCall, the scattering atmosphere viewed in Hα would be oblate while it would be prolate at the wavelength of the Ca II triplet.

7.4 THE SPECKLE COMPANION

Using speckle techniques, Karovska *et al.* (1987) made the fascinating discovery [confirmed by Matcher, Meikle & Morgan (1987)] of a source of emission close to SN 1987A not present before the explosion. If this companion source is physically associated with the supernova we might expect its observed position angle to be related to that derived for the polarization.

7.4.1 Comparison with the polarization data

A simple model of the supernova polarization consisting of some distribution of scattering material with a single well-defined symmetry axis would result in polarization lying on a line in the QU plane. This would be true, independent of how much interstellar polarization is present. The actual situation is more confusing because the observations do not define a line in the QU plane and show apparently different behaviour depending on the epoch and wavelength of the observations. Early broad-band observations from Cropper *et al.* (1987) and Bailey *et al.* (1987) define a line corresponding to a position angle of 129°±6.5, whereas the June 3 spectropolarimetry for the 5800 Å-region defines a line at close to 0° (Fig. 17g). However, when all the spectropolarimetric data are plotted on a single QU diagram (Fig. 17h) they define, not a line, but a broad band corresponding to a position angle of 16.5°±3. This is identical, within the uncertainties, to the position angle measured for the speckle companion.

The band in the QU plane extends on either side of the likely interstellar polarization value, indicating polarization both perpendicular and parallel to the speckle source position angle (since

180° in the QU plane corresponds to 90° in position angle). It seems likely that the angle defined by this band is the principal symmetry axis of the supernova envelope. Thus the data support a physical association between the speckle companion and the supernova itself, rather than a model in which the companion is a cloud of material being illuminated by the supernova. Alternatively our data would be consistent with a model in which the supernova produces a well-defined beam of radiation which illumines only a small region of the surrounding material.

7.4.2 The polarization of the speckle source

According to both Karovska *et al.* (1987) and Matcher *et al.* (1987), the companion was ~3 mag fainter at Hα than the supernova. This is a factor of ~15. As pointed out by Phinney (1987), if the source was 100 per cent polarized in this band (100 and 10 Å respectively for the two observations), the observed polarization would be ~6.5 per cent. As the flux-weighted polarization (corrected by our adopted value for the interstellar component) between 6500 and 6600 Å is ~0.4 per cent in both our March 7 and May 5 observations (thus bracketing the speckle observations), the intrinsic polarization of the companion itself can at most (when all the intrinsic polarization measured for SN 1987A is attributed to the companion) be 6 per cent. This conclusion does depend on the value adopted for the interstellar polarization; however, for reasonable values the upper limit is still $\lesssim$9 per cent.

Because the polarization is strongly modulated as a function of wavelength (Figs 2 to 15) and because the scattering axes for Hα and the Ca II triplet are perpendicular (Section 7.3.5), any intrinsic polarization of the companion cannot be the major source of the supernova polarization. Similarly, the loops in the QU plane denoting the loci of the polarization as a function of wavelength and the perpendicularity of the axes referred to above also exclude scattering of the supernova light from the companion as the major source of the supernova polarization. It is clear therefore that the polarization observed for SN 1987A is principally caused by scattering from its own atmosphere.

8 Conclusions

We have presented a large quantity of spectropolarimetric data with high S/N ratios showing the evolution of particular features with time and providing wide wavelength coverage at later epochs. Numerous polarization features are evident in the spectra. These are intrinsic to SN 1987A and we therefore conclude that its scattering atmosphere is not spherically symmetric. The shape of the atmosphere and principal scattering axis is wavelength-dependent. These principal axes are perpendicular to each other for the Hα line and Ca II infrared triplet. We have also compared the observed polarizations with those predicted by existing published models, for example those of Shapiro & Sutherland (1982) and McCall (1984). Axial ratios of ~0.8 to 0.9 are predicted for scattering atmospheres which are oblate spheroids. The observations are at odds with some of the predictions of these models and more detailed theoretical modelling is obviously required.

We have discussed the interstellar component in some detail and its effect on the measured polarization. The best estimate of this component is 0.7 per cent at 25°.

We find that the locus of the polarization data in the QU plane defines a band aligned along the same position angle as that to the speckle companion observed by Karovska *et al.* (1987) and Matcher *et al.* (1987). This suggests a physical association between the supernova and the speckle source.

Availability

The observations presented in this paper are available, already reduced in FITS format, to any investigator requiring them. Requests should be addressed to The Director, Anglo-Australian Observatory.

Acknowledgments

These observations could not have been made without the dedicated support of the technical staff at the AAT. The endless instrument changes and the spectropolarimeter modifications required a close attention to detail; they were done successfully despite an already overcrowded schedule. We are grateful to those observers who were displaced and to the committees responsible for allocation of telescope time for providing the necessary flexibility for these observations to be carried out. We are also grateful to David Allen and Bruce Margon for helpful discussions. MC was supported by an SERC AAO Fellowship and WJC by an Australian National Research Fellowship.

References

Bailey, J. A., Cannon, R. D. & Cropper, M. S., 1987. *IAU Circ. No. 4404.*
Bailey, J. A., Ogura, K. & Sato, S., 1987. *IAU Circ. No. 4351.*
Barrett, P., 1987a. *IAU Circ. No. 4337.*
Barrett, P., 1987b. *IAU Circ. No. 4340.*
Branch, D., 1980. In: *Supernova Spectra,* p. 39, eds Meyerott, R. E. & Gillespie, G. H., American Institute of Physics, New York.
Chandrasekhar, S., 1960. *Radiative Transfer,* Dover Publications.
Condon, E. U. & Shortley, G. H., 1964. *The Theory of Atomic Spectra,* Cambridge University Press.
Couch, W. J., Taylor, K., McCowage, J., Bailey, J. A. & Cropper, M. S., 1987. *IAU Circ. No. 4358.*
Cropper, M. S., Bailey, J. A., Peacock, T. I. & Wickramasinghe, D. T., 1987. *IAU Circ. No. 4319.*
Danziger, I. J., Fosbury, R. A. E., Alloin, D., Cristiani, S., Dachs, J., Gouiffes, C., Jarvis, B. & Sahu, K. C., 1987. *Astr. Astrophys.,* **177,** L13.
Dyson, J. E. & Meaburn, J., 1971. *Astr. Astrophys.,* **12,** 219.
Feast, M. W., 1986. *Galaxy Distances and Deviations from Universal Expansion*, p. 7, eds Madore, B. F. & Tully, R. B., Reidel, Dordrecht, Holland.
Karovska, M., Nisenson, P., Noyes, R. & Papaliolios, C., 1987. *IAU Circ. No. 4382.*
McCall, M. L., 1984. *Mon. Not. R. astr. Soc.,* **210,** 829.
McCall, M. L., Reid, N., Bessell, M. S. & Wickramasinghe, D. T., 1984. *Mon. Not. R. astr. Soc.,* **120,** 838.
McLean, I. S., Heathcote, S. R., Paterson, M. J., Fordham, J. & Shortridge, K., 1984. *Mon. Not. R. astr. Soc.,* **209,** 655.
McKenna, S. J., 1984. *Astrophys. Space Sci.,* **107,** 61.
Magalhaes, A. M. & Velloso, E. W., 1987. *IAU Circ. No. 4361.*
Martin, P. G., 1978. *Cosmic Dust: Its Impact on Astronomy,* Oxford University Press.
Matcher, S. J., Meikle, P. S. & Morgan, B. L., 1987. *IAU Circ. No. 4391.*
Mathewson, D. S. & Ford, V. L., 1970. *Astr. J.,* **75,** 778.
Phinney, E. S., 1987. Preprint.
Poeckert, R., 1982. *Proc. IAU Symp. No. 98,* p. 453, eds Jaschek, M. & Groth, H.-G., Reidel, Dordrecht, Holland.
Poeckert, R. & Marlborough, J. M., 1978. *Astrophys. J.,* **220,** 940.
Schmidt, Th., 1976. *Astr. Astrophys. Suppl.,* **24,** 357.
Schwarz, H. E. & Mundt, R., 1987. *Astr. Astrophys.,* **177,** L4.
Serkowski, K., 1974. In: *Planets, Stars and Nebulae Studied with Photopolarimetry,* p. 170, ed. Gehrels, T., University of Arizona Press, Tucson, USA.
Shapiro, P. R. & Sutherland, P. G., 1982. *Astrophys. J.,* **263,** 902.
Walsh, J. R., Bailey, J. A. & Ogura, K., 1987. *IAU Circ. No. 4328.*
West, R. M., Lauberts, A., Jørgensen, H. E. & Schuster, H.-E., 1987. *Astr. Astrophys.* **177,** L1.